Revisiting Theoretical Description of the Retrograde Motion of Cathode Spots of Vacuum Arcs

Mikhail S. Benilov, Helena T. C. Kaufmann, Werner Hartmann, and Larissa G. Benilova

***Abstract*— A fresh attempt to develop a self-consistent description of the retrograde motion of cathode spots on volatile cathodes is undertaken. Three potential mechanisms of effect of transversal magnetic field on the distribution of parameters in the spot are studied: the effect of magnetic field on hydrodynamics processes in the spot, in particular, on the formation of liquid-metal jet and the droplet detachment, and the effect of transversal magnetic field over the motion of ions and emitted electrons in the near-cathode space-charge sheath. It is found that for typical conditions of cathode spots in vacuum arcs the effect of magnetic field over the formation of liquid-metal jet and the droplet detachment is negligible; the motion of the ions in the near-cathode space-charge sheath is not disturbed; and the motion of the emitted electrons is disturbed only marginally. Thus, the above-mentioned potential mechanisms are hardly relevant and the first-principle understanding is still missing. A phenomenological description of the retrograde motion is developed as an alternative. The description employs general considerations without relying on specific assumptions and the (only) unknown parameter can be determined from comparison with the experiment.**

***Index Terms*— Arc discharges, cathodes, plasma sheaths, vacuum arcs.**

I. Introduction

When a transversal magnetic field is present, current spots on arc cathodes made of volatile metals move predominantly in the anti-Amperian, or "retrograde", direction. One of the consequences is that neighboring spots tend to repel, rather than attract, each other. The retrograde motion of current spots on volatile cathodes of arc discharges and, in particular, the repulsion of neighboring spots is a phenomenon of high theoretical interest and importance for applications. In particular, it contributes to preventing the merger of individual spots on negative contacts of high-power vacuum circuit breakers, which would result in the appearance of destructive arc attachments with currents of tens of kiloamperes.

The retrograde motion of cathode arc spots was discovered over one hundred years ago [1] and a number of theoretical models based on some or other assumptions have been published, e.g., [2]–[14]. In particular, it has been understood that, since "motion" of arc spots on volatile cathodes represents a sequence of extinctions followed by reignitions at neighboring locations, the direction of motion being retrograde means that the azimuthal distribution of probability of reignition at a particular position with respect to the extinct spot is anisotropic and has a maximum on the anti-Amperian side of the extinct spot. Thus, understanding the mechanism of retrograde motion amounts to explaining the reason for anisotropy of the azimuthal distribution of probability of reignition of a spot with a maximum on the anti-Amperian side. However, the first-principle understanding is still missing, although explanations based on various more or less arbitrary assumptions are abundant.

Important advances have been achieved recently in the modeling of cathode spots in vacuum arcs [15]–[22]. It is natural to revisit the question of retrograde motion in light of these advances in the hope to move closer to the first-principle understanding.

The appropriate first step would be to study the effect of transversal magnetic field on the distribution of parameters in the spot. The net transversal magnetic field in the spot represents a superposition of the external and self-generated fields, and is the highest on the anti-Amperian side of the spot and the lowest on the Amperian side. Therefore, if an effect of transversal magnetic field is found, it would mean that the azimuthal distribution of spot parameters is anisotropic, and in particular, spot parameters on the Amperian side of the spot differ from those on the anti-Amperian side. The second step will be to relate the anisotropy to the retrograde motion.

Three potential mechanisms of the effect of transversal magnetic field on the distribution of parameters in the spot are studied in this paper. The effect of magnetic field on hydrodynamics processes in the spot, in particular, on the formation of liquid-metal jet and the droplet detachment, is discussed in Section II. The second and third mechanisms, discussed in Section III, are the effects of transversal magnetic field over the motion in the near-cathode space-charge sheath of ions and emitted electrons, respectively.

It is found that, for the typical conditions of cathode spots in vacuum arcs, the effect of magnetic field over the formation of liquid-metal jet and the droplet detachment is negligible; the motion of ions is not disturbed; and the motion of the emitted

Manuscript received December 26, 2018; accepted February 26, 2019. Date of publication May 27, 2019; date of current version August 9, 2019. This work was supported in part by FCT–Fundação para a Ciência e a Tecnologia of Portugal under Project Pest-OE/UID/FIS/50010/2013 and in part by Siemens AG. The review of this paper was arranged by Senior Editor K. W. Struve. *(Corresponding author: Mikhail S. Benilov.)*

M. S. Benilov and H. T. C. Kaufmann are with the Departamento de Física, Faculdade de Ciências Exatas e da Engenharia, Universidade da Madeira, 9000 Funchal, Portugal, and also with the Instituto de Plasmas e Fusão Nuclear, Instituto Superior Técnico, Universidade de Lisboa, 1049 Lisbon, Portugal (e-mail: benilov@staff.uma.pt).

W. Hartmann, deceased, was with Siemens AG, Corporate Technology, 91058 Erlangen, Germany.

L. G. Benilova is with the Departamento de Física, Faculdade de Ciências Exatas e da Engenharia, Universidade da Madeira, 9000 Funchal, Portugal.

Color versions of one or more of the figures in this paper are available online at http://ieeexplore.ieee.org.

Digital Object Identifier 10.1109/TPS.2019.2904866

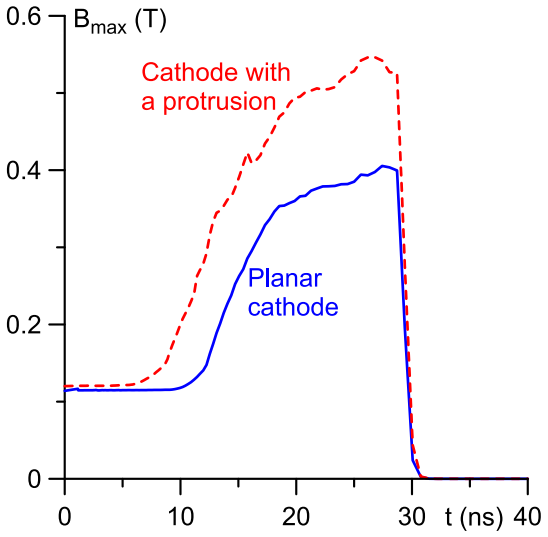

Fig. 1. Maximum value of magnetic field generated in a spot on a copper cathode of vacuum arc.

electrons is disturbed only on the periphery of the spot. Thus, the three above-mentioned potential mechanisms are hardly relevant and the first-principle understanding still remains elusive. In Section IV, a phenomenological description of the retrograde motion is developed as an alternative. Conclusions are briefly summarized in Section V.

II. Effect of Magnetic Field on the Formation of Liquid-Metal Jet and the Droplet Detachment

Unfortunately, 3-D modeling of cathode spots, which is needed to accurately simulate the effect of external transversal magnetic field over the distribution of parameters in cathode spots, is hardly feasible at present; note that the above-mentioned simulations [15]–[22] have been performed in the approximation of axial symmetry. However, a simplified approach is possible: one can study the effect produced on the distribution of parameters of a spot by the self-generated transversal magnetic field alone, without any external transversal magnetic field; if an effect has been found, one will be able to estimate the anisotropy of the distribution of parameters in the spot introduced by the interaction of the self-generated and external magnetic fields.

In this paper, the effect produced by the self-generated transversal magnetic field over hydrodynamics processes in the spot by is studied numerically with the use of the model of cathode spots in vacuum arcs [20]. The model takes into account all the potentially relevant mechanisms: the bombardment of the cathode surface by ions coming from a preexisting plasma cloud; vaporization of the cathode material in the spot, its ionization and the interaction of the produced plasma with the cathode; the Joule heat generation in the cathode body; melting of the cathode material and motion of the melt under the effect of the plasma pressure and the Lorentz force and related phenomena.

The computed evolution of the maximum value (in space) of self-generated magnetic field is shown in Fig. 1 for two copper cathodes, one of which was initially (before the spot occurrence and the formation of a crater) planar and the other

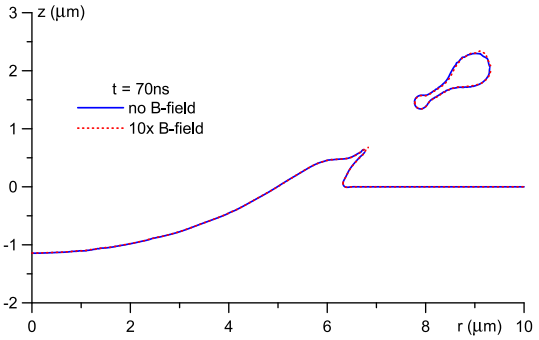

Fig. 2. Droplet detachment in a spot on copper cathode of vacuum arc.

had initially a microprotrusion, see [20] for more details. The maximum magnetic field is the highest and attains values around $0.4 - 0.5\,\mathrm{T}$ at $t = 25\,\mathrm{ns}$, right before the pre-existing plasma cloud is extinguished. Note that the spot current at $t = 25\,\mathrm{ns}$ is the highest as well, around $10 - 12\,\mathrm{A}$ [20].

In order to obtain an upper estimate of the effect of magnetic field on hydrodynamics processes in the spot, two sets of simulations have been performed: without an account of the self-generated magnetic field and with the self-generated magnetic field amplified by a factor of ten. As an example, the shape of the cathode and the droplet at the moment $t = 70\,\mathrm{ns}$, soon after the droplet detachment, is shown in Fig. 2 for the case of planar cathode. The solid and dotted lines, representing the results of simulations performed without an account of the self-generated magnetic field and with the self-generated magnetic field amplified by a factor of ten, respectively, coincide. Thus, the effect of self-generated magnetic field over the formation of liquid-metal jet and the droplet detachment is negligible.

III. Effect of Magnetic Field on the Motion of Charged Particles in the Space-Charge Sheath

A. Effect on the Motion of the Ions

The effect of magnetic field on the motion of the ions in the space-charge sheath was studied by means of introducing an account of transversal magnetic field into the classic Child–Langmuir ion sheath model. In the framework of this model, the effect of transversal magnetic field over the ion motion may be characterized by the dimensionless control parameter $\theta_i = (\varepsilon_0 e B^2/m_i j_i)(eU/m_i)^{(1/2)}$ (all designations here and further are conventional), which represents the squared ratio of the Debye length, evaluated in terms of the electrostatic energy instead of the electron thermal energy, to the characteristic ion Larmor radius.

The theory of Child–Langmuir ion sheath with a transversal magnetic field is rather trivial, however, seems to be absent in the literature. For completeness, it is briefly given in Appendix A. Computed trajectories of the ions are shown in Fig. 3 for several values of θ_i. [Here, ξ and ζ are coordinates normalized by $(\varepsilon_0^2 eU^3/m_i j_i^2)^{1/4}$.] The trajectory becomes tangent to the cathode surface for $\theta_i \approx 4.443$.

B. Effect on the Motion of the Emitted Electrons

The effect of magnetic field over electrons, emitted by the cathode surface in the Child–Langmuir sheath, may be

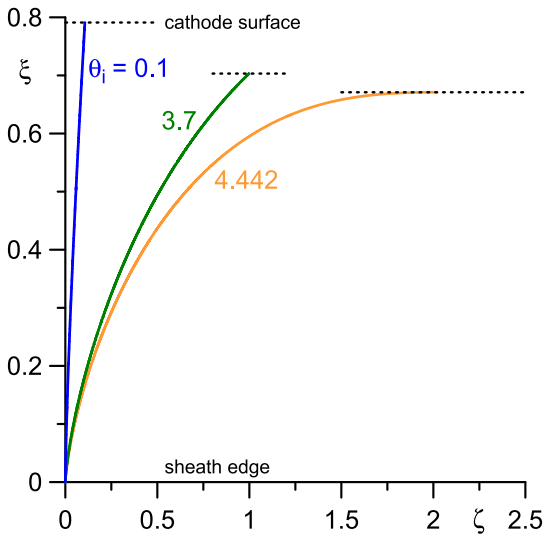

Fig. 3. Trajectories of the ions in the Child–Langmuir ion sheath with transversal magnetic field.

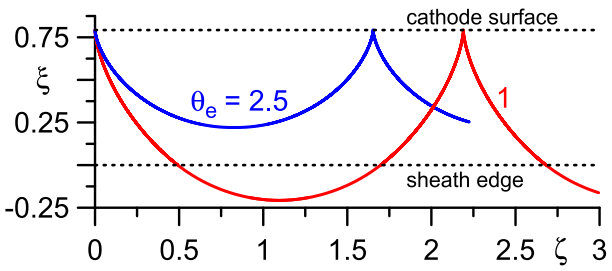

Fig. 4. Trajectories of the emitted electrons in the Child–Langmuir sheath.

characterized by the dimensionless parameter θ_e, which represents the squared ratio of the Debye length, evaluated in terms of the electrostatic energy, to the characteristic electron Larmor radius, and is related to θ_i as $2\theta_e/\theta_i = m_i/m_e \gg 1$. The motion of electrons in the sheath starts being affected by the magnetic field in the case where θ_e is comparable to unity. Since θ_i is very small in this case, the ion motion and the distribution of electrostatic potential in the sheath are not perturbed by the presence of magnetic field in this case.

The trajectories of emitted electrons are found in Appendix B. The emitted electrons are confined in the sheath for $\theta_e \gtrsim 1.591$. As an example, the trajectory of emitted electrons for $\theta_e = 2.5$ is shown in Fig. 4. For $\theta_e < 1.591$, a part of each trajectory is positioned outside the sheath (in the region $\xi < 0$), as exemplified by the trajectory for $\theta_e = 1$.

C. Estimates for Cathode Spots of Vacuum Arcs

As far as space-charge sheaths near cathodes of vacuum arcs are concerned, the important question is where the ions forming the sheath originate in. One should distinguish between two cases. The first is the case where the ions originate in outside the spot, e.g., from the background bulk plasma or the plasma cloud produced by the previous spot (a spot that has existed previously in the vicinity of the point on the cathode surface being considered). The second is the case where the ions are generated at the expense of the energy of electrons emitted from the cathode inside the currently existing spot and accelerated by the sheath electric field. For example, the ions may originate in the ionization of neutral atoms evaporated inside the currently existing spot (which occurs in the ion–electron layer or in the quasi-neutral plasma immediately outside the ion–electron layer; the so-called ionization layer); or from the ionization of neutral atoms of a cloud produced by the previous spot.

The relevant parameter in the first case is θ_i. Assuming that the ions enter the near-cathode space-charge sheath with Bohm's velocity, the density of ion current to the cathode surface can be expressed as $j_i = en_e^{(q)}(kT_e/m_i)^{(1/2)}$, where $n_e^{(q)}$ is the characteristic electron density in the bulk plasma or the plasma cloud produced in the previous spot. The expression for θ_i may be rewritten as

$$\theta_i = \frac{\varepsilon_0 B^2}{m_i n_e^{(q)}}\sqrt{\frac{eU}{kT_e}}. \tag{1}$$

Let us assume that the cathode material is copper and the transversal magnetic field is 1 T. (This is the value of magnetic field induced by a spot carrying current of 50 A at 10 μm from the spot center.) Assuming 2 eV as a typical electron temperature and 20 V as a typical sheath voltage, one can rewrite (1) in the dimensionless form as $\theta_i = 2.7\times10^{14}\,\mathrm{m}^{-3}/n_e^{(q)}$. Values of the electron density $n_e^{(q)}$ of $10^{20}\,\mathrm{m}^{-3}$ and $10^{26}\,\mathrm{m}^{-3}$ may be assumed as characteristic for the bulk plasma and the plasma cloud left over from the previous spot, respectively. Then, θ_i is of the order of 10^{-6} for the bulk plasma and 10^{-12} for the plasma cloud left over from the previous spot. Hence, the effect of magnetic field is negligible in the case of ions entering the sheath from the bulk plasma or the plasma cloud produced in the previous spot; an understandable result related to the smallness of the Hall number for the ions.

Let us proceed to the second case, where the source of ionization energy is the energy of electrons emitted inside the spot. The relevant parameter is θ_e. Assuming $B = 1\,\mathrm{T}$ and $U = 20\,\mathrm{V}$ as above, one can rewrite the expression for θ_e for copper in the dimensionless form as $\theta_e = 0.86\times10^4\,\mathrm{A\,m^{-2}}/j_i$.

Let us assume that the ions originate in the ionization of neutral atoms evaporated inside the currently existing spot, and employ the model of near-cathode plasma layers described in [23]. Parameters of the near-cathode layer and, in particular, the ion current to the cathode are governed in this model by the temperature T of cathode surface and the near-cathode voltage drop U. Note that although the near-cathode voltage drop in the model [23] is not defined in the same way as in the Child–Langmuir model, the two definitions coincide to the accuracy of the order of kT_e.

As an example, dependences of the ion current density $j_i(T)$, parameter $\theta_e(T)$, and the sheath thickness $d(T)$ are shown in Fig. 5 for $U = 20\,\mathrm{V}$. Note that the sheath thickness d in this case is not affected by the presence of magnetic field and is related to the length scale $\delta = \left(\varepsilon_0 U/en_i^{(s)}\right)^{(1/2)}$ (see Appendix A) as $d = (2^{5/4}/3)\delta$. The value of T at which the ion current density equals $0.86\times10^4\,\mathrm{A\,m^{-2}}$ and θ_e equals unity is approximately 2490 K.

One needs information on the distribution of cathode surface temperature inside the spot in order to identify the point at which the above-mentioned value of 2490 K occurs and

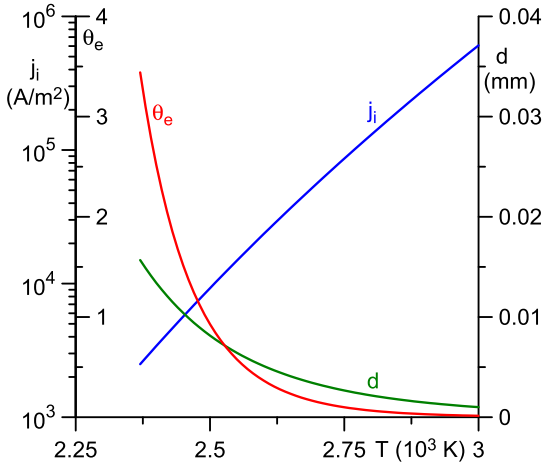

Fig. 5. Parameters of sheath on copper cathode of vacuum arc. U=20 V. Evaluation by means of the model [23].

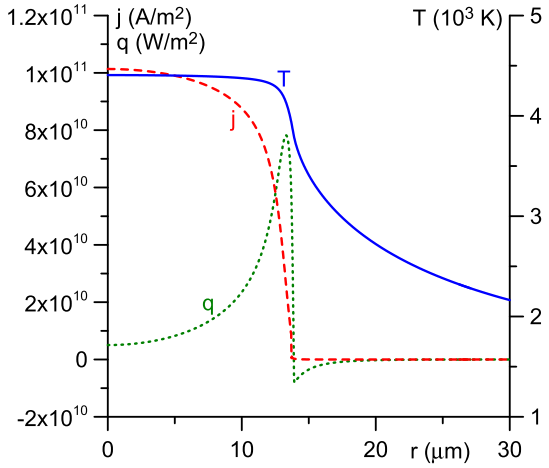

Fig. 6. Computed distributions of parameters in a steady-state spot on copper cathode of vacuum arc. U=20 V. Solid: temperature of the surface. Dashed: electric current density. Dotted: density of energy flux from the plasma to the cathode surface. Model [24].

$\theta_e = 1$. As the first example, let us consider results of space-resolved calculations of steady-state spots on planar copper cathodes [24], as shown in Fig. 6. The point with the above-mentioned temperature value of 2490 K is positioned at $r \approx 23\,\mu$m from the spot center. Note that the ion current density at the spot center is approximately $10^{10}\,\mathrm{A\,m^{-2}}$.

As another example, let us consider the distribution of cathode surface temperature given by the model of transient cathode spots in vacuum arcs ignited by a pre-existing plasma cloud [20], which has already been employed in the analysis of Section II. The temperature distributions along the surface of a copper cathode, which was initially (before the spot occurrence) planar, are shown in Fig. 7 for two subsequent moments, $t = 20$ and 25 ns. Here, r is the distance from the spot center measured along the cathode surface (which is not planar at these moments since the crater has already been formed, see [20, Fig. 3(a)]). The point with the above-mentioned temperature value of 2490 K is positioned at the distance $r \approx 5.1\,\mu$m from the spot center for $t = 20$ ns and at $r \approx 5.8\,\mu$m for $t = 25$ ns. The ion current density at the spot

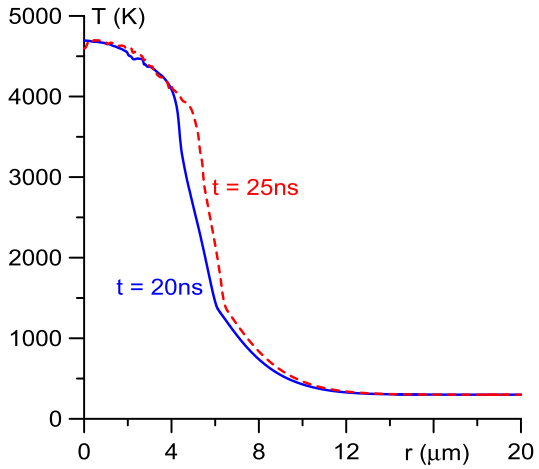

Fig. 7. Computed distributions of surface temperature in a transient spot ignited by a pre-existing plasma cloud on copper cathode of vacuum arc; model [20].

center is approximately $1.7 \times 10^{10}\,\mathrm{A\,m^{-2}}$ for $t = 20$ ns and $1.4 \times 10^{10}\,\mathrm{A\,m^{-2}}$ for $t = 25$ ns.

The two above-mentioned examples are very different in that the model [24] describes a stationary spot on a planar cathode without regard of the motion of the molten cathode material, whereas the model [20] describes a transient spot ignited by a pre-existing plasma cloud and takes into account the motion of the molten cathode material and the change of shape of the surface due to this motion. Accordingly, the point where $\theta_e = 1$ is positioned at different distances from the spot center, $r = 23\,\mu$m and r between 5 and 6 μm, respectively. However, the ion current density at this point in both cases is by six orders of magnitude lower than that at the spot center. Note that the sheath thickness at this point, evaluated by means of the model of near-cathode layers [23], is $d \approx 8.6\,\mu$m; the net current density is $1.6 \times 10^4\,\mathrm{A\,m^{-2}}$; the ionization degree of plasma is 0.86×10^{-3}; the ion backflow coefficient is 4.3×10^{-4}; the density of ion energy flux to the cathode is $2 \times 10^5\,\mathrm{W\,m^{-2}}$, which is five times higher than the electron emission cooling but by two orders of magnitude smaller than the vaporization cooling.

One can conclude that in both examples the effect of transversal magnetic field on the motion of the emitted electrons in the near-cathode space-charge sheath comes into play at a periphery of the spot and can hardly play a role in the retrograde motion.

IV. Phenomenological Description of the Retrograde Motion

Summarizing results of Sections II and III, one can conclude that the first-principle understanding of the retrograde motion of cathode spots of vacuum arcs still remains elusive, in spite of important advances achieved recently in the modeling of cathode spots in vacuum arcs. One of the two remaining options is to invoke an assumption, which, however, cannot but be arbitrary. The other option is to try to develop a phenomenological description or, in other words, to use general considerations without relying on specific assumptions and then to determine unknown parameter(s) from comparison with the experiment.

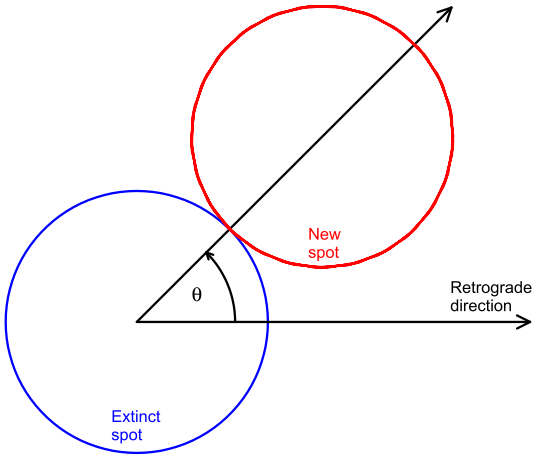

Fig. 8. Schematic of subsequent positions of a spot.

Let us designate by $\psi(\theta)$ the probability of ignition of a new spot at an azimuthal angle θ with respect to the position of the initial spot, with $\theta = 0$ being attributed to the retrograde direction (Fig. 8). Two cases are possible: the one where $\psi(\theta)$ varies significantly, that is, the distribution of probability is substantially anisotropic, and the one where the function $\psi(\theta)$ is close to a constant, that is, the distribution of ignition probability is nearly isotropic. In the first case, the spot is displaced over a distance of the order of spot diameter in the direction $\theta = 0$ during each lifecycle. Hence, in this case, the speed of the retrograde motion, v_r, will be of the order of $2R/\Delta t$, where R is the spot radius and Δt is the residence time of the spot. In the second case, where the distribution of probability is nearly isotropic, v_r will be much smaller than $2R/\Delta t$.

Assuming as characteristic values $R = 10\,\mu$m and $\Delta t = 50$ ns, one obtains $2R/\Delta t = 400\ \text{m s}^{-1}$. This value is much higher than speed of the retrograde motion observed in the experiment, which normally does not exceed $20 - 30\,\text{m s}^{-1}$, e.g., see [25]. Hence, the second case is the realistic one, that is, the distribution of probability is nearly isotropic.

It follows that the function $\psi(\theta)$ may be represented as

$$\psi(\theta) = \psi_0 + \psi_1(\theta) \tag{2}$$

where ψ_0 is a constant describing the isotropic part of the ignition probability and $|\psi_1(\theta) \ll 1|$. ψ_0 may be found from the normalization condition: $\psi_0 = 1/2\pi$. It is legitimate to assume that $\psi_1(\theta)$ is linear with respect to the factor perturbing the isotropy, which is the interaction between the external transversal magnetic field and the azimuthal magnetic field generated by the (initial) spot. Let us designate by $\mathbf{B}_0$ the external magnetic field and by $\mathbf{B}_s$ the self-generated magnetic field estimated, say, at the spot edge. The simplest scalar quantity characterizing two vectors is their scalar product. Therefore, $\psi_1(\theta) = A\mathbf{B}_0 \cdot \mathbf{B}_s$, where A is an unknown parameter. Evaluating $\mathbf{B}_s$ in terms of the spot current I and radius R, one finds $\mathbf{B}_0 \cdot \mathbf{B}_s = B_0(\mu_0 I/2\pi R)\cos\theta$. Thus, (2) can be rewritten as

$$\psi(\theta) = \frac{1}{2\pi} + \frac{aB_0}{2\pi R}\cos\theta \tag{3}$$

where $a = A\mu_0 I$ is a new parameter. Note that the right-hand side (RHS) of (3) may be viewed as sum of the first and second terms of the Fourier series of the function $\psi(\theta)$. In order that the extremum that the RHS has at $\theta = 0$ (on the anti-Amperian side) to be a maximum, parameter a must be positive.

Thus, the retrograde motion can be described by (3), which is supposed to be of a general nature and, therefore, should be valid regardless of the actual mechanism of the retrograde motion. The speed v_r of the retrograde motion is expressed from this equation as $v_r = aB_0/\Delta t$.

Understanding of the mechanism of retrograde motion is indispensable in order to theoretically determine coefficient a. On the other hand, a may be determined empirically. For example, the measurements [25] have given $v_r = 260 B_0\,\text{m s}^{-1}\,\text{T}^{-1}$ for the following conditions: $I = 65...245$ A, $B_0 \lesssim 0.08$ T, CuCr30 cathode, and the interelectrode gap of 2 mm. Assuming $\Delta t = 50$ ns as above, one finds $a = 1.3 \times 10^{-5}\,\text{m T}^{-1}$ for these conditions.

Using these numerical values and assuming $R = 10\,\mu$m as above and $B_0 = 0.1$ T, one can rewrite (3) as

$$\psi(\theta) = \frac{1}{2\pi}(1 + 0.13\cos\theta). \tag{4}$$

The second term in the parentheses on the RHS does not exceed 13% of the first term, that is, the anisotropy is small as expected.

V. Conclusion

A fresh attempt to find a first-principle explanation of the retrograde motion of arc spots on cathodes made of volatile materials is undertaken with the use of advances achieved recently in the modeling of cathode spots in vacuum arcs. Three potential mechanisms of the effect of transversal magnetic field on the distribution of parameters in the spot have been studied: the effect of magnetic field on hydrodynamic processes in the spot, in particular, on the formation of liquid-metal jet and the droplet detachment; the effect of transversal magnetic field over the motion of ions in the near-cathode space-charge sheath; and the effect of transversal magnetic field over the motion of emitted electrons in the near-cathode space-charge sheath. However, all the three effects are found to be negligible. Thus, the first-principle understanding of the retrograde motion of cathode spots of vacuum arcs remains elusive.

A phenomenological description of the retrograde motion of cathode spots in vacuum arcs has been developed as an alternative. The description employs general considerations without relying on specific assumptions and the (only) unknown parameter can be determined from comparison with the experiment.

Appendix A
Child–Langmuir Ion Sheath With Magnetic Field

Let us consider a collisionless space-charge sheath adjacent to the cathode of a gas discharge in the limiting case $U \gg kT_e/e$, where U is the sheath voltage, and kT_e is the thermal energy of the plasma electrons. The sheath may be divided into two zones: the bulk of the sheath, where the plasma electrons cannot penetrate, and the outer section of the sheath, where the density of plasma electrons, while being different from the ion density, is still comparable to the latter.

The latter zone will be referred to as the ion–electron layer and the former as the ion layer. The appropriate mathematical description of these zones may be obtained by means of the method of matched asymptotic expansions treating the ratio $\chi = eU/kT_e$ as a large parameter; asymptotic estimates of scales of relevant parameters in each of these zones may be found in [26].

In the classic Bohm model [27], the case is considered where the ion flux to the cathode is generated in the quasi-neutral plasma: the ions enter the sheath from the quasi-neutral plasma and then are accelerated in the direction to the cathode. In [28], the case is considered where the ion flux to the cathode is generated in the ion–electron layer. This case is relevant for vacuum arcs and is of interest also for this paper. Although the physics of the ion–electron layer is different in the two cases, asymptotic scalings of relevant parameters in the layer with respect to χ are the same. On the other hand, the physics of the ion layer in both cases is the same and the ion layer to the first approximation in the parameter χ^{-1} is described by the same model: the classical Child–Langmuir sheath model.

In addition to the plasma electrons, there may also be present electrons emitted by the cathode surface, so net current to the cathode surface represents the sum of current of ions coming to the surface and of electrons emitted by the surface. Assuming that the ion current amounts to 10% or more of the net current and taking into account that the speed of electrons exceeds the speed of ions, accelerated by the same potential difference, by a factor of 100 or more, one should conclude that the contribution of emitted electrons to the space charge in the sheath does not exceed 10%. Neglecting this contribution, one can decouple the problem: first, the ion density and the electric field are found by solving the Child–Langmuir problem, after which the acceleration of the emitted electrons in the known electric field is considered.

In this Appendix, the effect of transversal magnetic field over the distribution of the ions and the electric field in the ion layer is studied. The effect of magnetic field over the emitted electrons is considered in Appendix B.

Let us formulate the problem governing the ion layer in the case where the uniform magnetic field parallel to the cathode surface is present. The scale of thickness of the ion layer is much bigger than the scale of thickness of ion–electron layer, therefore, one can speak of an "edge" of the ion layer. The x-axis is directed from the edge to the cathode surface. The magnetic field is directed along the y-axis: $\mathbf{B} = (0, B, 0)$. The ion velocity may be represented as $\mathbf{v}_i = (u, 0, w)$. Distribution of parameters in the ion layer is governed by the following equations:

$$m_i u \frac{du}{dx} = -e\frac{d\varphi}{dx} - ewB, \quad m_i u \frac{dw}{dx} = euB, \tag{5}$$

$$j_i = en_i u, \quad \varepsilon_0 \frac{d^2\varphi}{dx^2} = -en_i. \tag{6}$$

Here, m_i and n_i are the particle mass and number density of the ions, respectively, j_i is the density of electric current transported by the ions to the cathode, and φ is the electrostatic potential.

Boundary conditions at the sheath edge and the cathode surface read, respectively,

$$x = 0: \quad u = w = 0, \quad \varphi = 0 \quad \frac{d\varphi}{dx} = 0 \tag{7}$$

$$x = d: \quad \varphi = -U. \tag{8}$$

Here, d designates the thickness of the sheath and is a parameter to be found. The zero of potential is attributed to the sheath edge. The first, second, and fourth boundary conditions in (7) have a clear physical meaning: since characteristic ion speed and electric field in the ion–electron layer are much smaller than those in the ion layer, the ion speed and electric field at the edge of the ion layer may be set equal to zero while treating this layer.

The ion current density j_i and the sheath voltage U are considered as known (positive) quantities. Then, the five boundary conditions (7), (8) are just sufficient to determine four integration constants and the sheath thickness d. Hence, the model is complete. In the absence of magnetic field, this model coincides with the Child–Langmuir sheath model: the ions enter the sheath with a zero speed and are accelerated by the self-induced electric field in the direction to the cathode. The magnetic field deflects the ions, however, does not prevent them from reaching the cathode. The latter implies a limitation on the magnetic field: when B reaches a value at which u vanishes at the cathode surface, the model loses its validity.

Integrating the second equation in (5) and then the first equation and applying the first two boundary conditions (7), one obtains

$$w = \omega_i x, \quad u = \sqrt{-\frac{2e\varphi}{m_i} - (\omega_i x)^2} \tag{9}$$

where $\omega_i = eB/m_i$ is the ion gyrofrequency.

The Poisson equation, second equation in (6), may now be written in a form involving only one dependent variable, the electrostatic potential

$$\varepsilon_0 \sqrt{-\frac{2e\varphi}{m_i} - (\omega_i x)^2}\, \frac{d^2\varphi}{dx^2} = -j_i. \tag{10}$$

Let us introduce characteristic ion speed and number density in the ion layer, $u_i^{(s)} = (eU/m_i)^{(1/2)}$, $n_i^{(s)} = j_i/eu_i^{(s)}$; the Debye length evaluated in terms of $n_i^{(s)}$ with the electron thermal energy kT_e replaced by the electrostatic energy eU, $\delta = \left(\varepsilon_0 U/en_i^{(s)}\right)^{(1/2)}$; and the characteristic ion Larmor radius in the layer, $R_L = u_i^{(s)}/\omega_i$. Equation (10) and the corresponding boundary conditions may be conveniently transformed to dimensionless variables $\xi = x/\delta$, $\Phi = -\varphi/U$

$$\sqrt{2\Phi - \theta_i \xi^2}\, \frac{d^2\Phi}{d\xi^2} = 1 \tag{11}$$

$$\xi = 0: \quad \Phi = 0, \quad \frac{d\Phi}{d\xi} = 0 \tag{12}$$

$$\xi = \Delta: \quad \Phi = 1 \tag{13}$$

where $\theta_i = (\delta/R_L)^2$ and $\Delta = d/\delta$. (Note that an alternative form of the former expression is $\theta_i = (\varepsilon_0 eB^2/m_i j_i)(eU/m_i)^{(1/2)}$.) One can see that the boundary-value problem (11)–(13) is governed by the single dimensionless control parameter θ_i, which characterizes the

effect of magnetic field. The above-described limitation of applicability of the model in terms of the magnetic field is now expressed in terms of θ_i: the model is valid for $\theta_i < \theta_0$, where θ_0 is the root of the transcendental equation

$$\Delta = \sqrt{2/\theta_i}. \tag{14}$$

After the boundary-value problem (11)–(13) has been solved, one can find trajectories of the ions. The trajectory that starts at the origin may be expressed as

$$\zeta = \sqrt{\theta_i}\int_0^{\xi} \frac{\xi}{\sqrt{2\Phi - \theta_i \xi^2}} d\xi \tag{15}$$

where $\zeta = z/\delta$. Using (11), this expression may be transformed to

$$\zeta = \sqrt{\theta_i}\left(\xi \frac{d\Phi}{d\xi} - \Phi\right). \tag{16}$$

The problem (11)–(13) was solved numerically. The singular point $\xi = 0$ was excluded from the domain of numerical integration with the use of the asymptotic expansion of solution of (11) subject to the boundary conditions (12) for the limiting case of small ξ, which reads

$$\Phi = C_1 \xi^{4/3} + C_2 \theta_i \xi^2 + C_3 \theta_i^2 \xi^{8/3} + \ldots \tag{17}$$

Here, $C_1 = (81/32)^{1/3}$, $C_2 = 1/20$, and $C_3 = 162^{2/3}/5600$. Note that the first term of this expansion represents the Child–Langmuir solution.

Results of the numerical calculations are shown in Fig. 3. The trajectory of an ion, shown in Fig. 3, becomes tangent to the cathode surface for $\theta_i = \theta_0 \approx 4.443$.

Appendix B
Emitted Electrons in the Child–Langmuir Space-Charge Sheath With Magnetic Field

Neglecting the kinetic energy with which the electrons are emitted from the cathode compared to the electrostatic energy eU, one obtains, similar to (9)

$$w_e = \omega_e \delta(\Delta - \xi), \quad u_e = -u_e^{(s)}\sqrt{1 - \Phi - \theta_e(\Delta - \xi)^2} \tag{18}$$

where $\omega_e = eB/m_e$ is the electron gyrofrequency, $u_e^{(s)} = (2eU/m_e)^{(1/2)}$ and $R_{Le} = u_e^{(s)}/\omega_e$ are the characteristic electron speed and Larmor radius, respectively, and $\theta_e = (\delta/R_{Le})^2$. (Note that alternative forms of the last expression are $\theta_e = (\varepsilon_0 e B^2/m_e j_i)(eU/m_i)^{(1/2)}$ and $\theta_e = \theta_i m_i/2m_e$.) In this section, we are concerned with the case where θ_e is of the order unity and, consequently, $\theta_i \ll 1$. Thus, the distribution of potential in the sheath is given by the first term of the expansion (17), $\Phi = C_1 \xi^{4/3}$, and the parameter Δ is given by the Child–Langmuir value, $\Delta = 2^{5/4}/3$.

Integrating equations (18) with the boundary condition $\zeta|_{\xi=\Delta} = 0$, one finds the first segment of the trajectory in the sheath (the one characterized by the decreasing dependence $\xi(\zeta)$) of electrons emitted from the point $(\xi = \Delta, \zeta = 0)$

$$\zeta = \sqrt{\theta_e}\Delta^2 \int_{\xi/\Delta}^{1} \frac{1 - r}{\sqrt{1 - r^{4/3} - \theta_e \Delta^2 (1 - r)^2}} dr. \tag{19}$$

The emitted electrons are confined in the sheath for $\theta_e \geq \theta_{cr} = \Delta^{-2} = 9 \times 2^{-5/2} \approx 1.591$. As an example, the trajectory of electrons emitted from the point $(\xi = \Delta, \zeta = 0)$ for $\theta_e = 2.5$ is shown in Fig. 4. Up to the first turning point, the trajectory is described by (19).

For $\theta_e < \theta_{cr}$, the trajectories are qualitatively similar, except for a part of each trajectory being positioned outside the sheath (in the region $\xi < 0$). Since the electric field outside the sheath is much lower than that inside the sheath, the trajectory outside the sheath is close to a circle of the electron Larmor radius R_{Le}. In the dimensionless variables, the radius of the circle is $\theta_e^{-1/2}$ and its center is positioned in the point $\left(\xi = \Delta, \zeta = \zeta_0 + \sqrt{\theta_e^{-1} - \Delta^2}\right)$. Here, ζ_0 designates the value of the coordinate ζ at which the emitted electron has left the sheath; for the first outside-the-sheath segment of the trajectory of electrons emitted from the point $(\xi = \Delta, \zeta = 0)$, ζ_0 is given by the integral (19) with $\xi = 0$. As an example, the trajectory for $\theta_e = 1$ is shown in Fig. 4 .

Acknowledgment

One of the authors passed away prematurely when this work was already at an advanced stage. His coworkers miss very much Werner Hartmann, a brilliant scientist and a dear friend.

References

[1] J. Stark, "Induktionserscheinungen am quecksilberlichtbogen im magnetfeld," *Physikal. Zeitschr*, vol. 4, pp. 440–443, 1903.
[2] A. E. Robson and V. A. Engel, "Origin of retrograde motion of arc cathode spots," *Phys. Rev.*, vol. 93, pp. 1121–1122, Mar. 1954. [Online]. Available: https://link.aps.org/doi/10.1103/PhysRev.93.1121.2
[3] D. Y. Fang, "Cathode spot velocity of vacuum arcs," *J. Phys. D: Appl. Phys.*, vol. 15, no. 5, p. 833, 1982. [Online]. Available: http://stacks.iop.org/0022-3727/15/i=5/a=013
[4] M. G. Drouet, "The physics of the retrograde motion of the electric arc," *IEEE Trans. Plasma Sci.*, vol. 13, no. 5, pp. 235–241, Oct. 1985.
[5] B. Y. Moizhes and V. A. Nemchinsky, "On the theory of the retrograde motion of a vacuum arc," *J. Phys. D: Appl. Phys.*, vol. 24, no. 11, p. 2014, 1991. [Online]. Available: http://stacks.iop.org/0022-3727/24/i=11/a=016
[6] A. Bolotov, A. Kozyrev, and Y. Korolev, "A physical model of the low-current-density vacuum arc," *IEEE Trans. Plasma Sci.*, vol. 23, no. 6, pp. 884–892, Dec. 1995. [Online]. Available: http://ieeexplore.ieee.org/xpl/articleDetails.jsp?arnumber=476470
[7] B. Jüttner and I. Kleberg, "The retrograde motion of arc cathode spots in vacuum," *J. Phys. D: Appl. Phys.*, vol. 33, no. 16, p. 2025, 2000. [Online]. Available: http://stacks.iop.org/0022-3727/33/i=16/a=315
[8] I. I. Beilis, "Vacuum arc cathode spot grouping and motion in magnetic fields," *IEEE Trans. Plasma Sci.*, vol. 30, no. 6, pp. 2124–2132, Dec. 2002.
[9] W. Hartmann and G. Lins, "Retrograde motion of cathode spots," in *Proc. 24th Int. Symp. Discharges Electr. Insul. Vac.*, Braunschweig, Germany, Aug./Sep. 2010, pp. 371–374.
[10] W. C. Lang, J. Q. Xiao, J. Gong, C. Sun, R. F. Huang, and L. S. Wen, "Study on cathode spot motion and macroparticles reduction in axisymmetric magnetic field-enhanced vacuum arc deposition," *Vacuum*, vol. 84, no. 9, pp. 1111–1117, 2010. [Online]. Available: http://www.sciencedirect.com/science/article/pii/S0042207X10000618
[11] M. M. Tsventoukh, S. A. Barengolts, G. A. Mesyats, and D. L. Shmelev, "Retrograde motion of cathode spots of the first type in a tangential magnetic field," *Tech. Phys. Lett.*, vol. 39, no. 11, pp. 933–937, 2013. doi: 10.1134/S1063785013110138.
[12] L. Li *et al.*, "Control of cathodic arc spot motion under external magnetic field," *Vacuum*, vol. 91, pp. 20–23, May 2013. [Online]. Available: http://www.sciencedirect.com/science/article/pii/S0042207X12004496
[13] Z. Shi, C. Wang, X. Song, S. Jia, and L. Wang, "Stepwise simulation on the motion of a single cathode spot of vacuum arc in external transverse magnetic field," *IEEE Trans. Plasma Sci.*, vol. 43, no. 1, pp. 472–479, Jan. 2015.
[14] I. I. Beilis, "A model of vacuum arc cathode spot motion in an oblique magnetic field," in *Proc. 27th Int. Symp. Discharges Electr. Insul. Vac.*, Suzhou, China, vol. 1, Sep. 2016, pp. 1–3.
[15] G. A. Mesyats and I. V. Uimanov, "Hydrodynamics of the molten metal during the crater formation on the cathode surface in a vacuum arc," *IEEE Trans. Plasma Sci.*, vol. 43, no. 8, pp. 2241–2246, Aug. 2015.

[16] M. A. Gashkov, N. M. Zubarev, O. V. Zubareva, G. A. Mesyats, and I. V. Uimanov, "Model of liquid-metal splashing in the cathode spot of a vacuum arc discharge," *J. Experim. Theor. Phys.*, vol. 122, no. 4, pp. 776–786, 2016.
[17] M. A. Gashkov, N. M. Zubarev, G. A. Mesyats, and I. V. Uimanov, "The mechanism of liquid metal jet formation in the cathode spot of vacuum arc discharge," *Tech. Phys. Lett.*, vol. 42, no. 8, pp. 852–855, 2016.
[18] M. D. Cunha, H. T. C. Kaufmann, M. S. Benilov, W. Hartmann, and N. Wenzel, "Detailed numerical simulation of cathode spots in vacuum arcs—I," *IEEE Trans. Plasma Sci.*, vol. 45, no. 8, pp. 2060–2069, Aug. 2017. doi: 10.1109/TPS.2017.2697005.
[19] G. A. Mesyats and I. V. Uimanov, "Semiempirical model of the microcrater formation in the cathode spot of a vacuum arc," *IEEE Trans. Plasma Sci.*, vol. 45, no. 8, pp. 2087–2092, Aug. 2017.
[20] H. T. C. Kaufmann, M. D. Cunha, M. S. Benilov, W. Hartmann, and N. Wenzel, "Detailed numerical simulation of cathode spots in vacuum arcs: Interplay of different mechanisms and ejection of droplets," *J. Appl. Phys.*, vol. 122, no. 16, p. 163303, 2017.
[21] X. Zhang, L. Wang, S. Jia, and D. L. Shmelev, "Modeling of cathode spot crater formation and development in vacuum arc," *J. Phys. D: Appl. Phys.*, vol. 50, no. 45, 2017, Art. no. 455203. [Online]. Available: http://stacks.iop.org/0022-3727/50/i=45/a=455203
[22] L. Wang, X. Zhang, Y. Wang, Z. Yang, and S. Jia, "Simulation of cathode spot crater formation and development on cucr alloy in vacuum arc," *Phys. Plasmas*, vol. 25, no. 4, 2018, Art. no. 043511. doi: 10.1063/1.5023213.
[23] N. A. Almeida, M. S. Benilov, L. G. Benilova, W. Hartmann, and N. Wenzel, "Near-cathode plasma layer on CuCr contacts of vacuum arcs," *IEEE Trans. Plasma Sci.*, vol. 41, no. 8, pp. 1938–1949, Apr. 2013. doi: 10.1109/TPS.2013.2260832.
[24] M. S. Benilov, M. D. Cunha, W. Hartmann, S. Kosse, A. Lawall, and N. Wenzel, "Space-resolved modeling of stationary spots on copper vacuum arc cathodes and on composite CuCr cathodes with large grains," *IEEE Trans. Plasma Sci.*, vol. 41, no. 8, pp. 1950–1958, 2013. doi: 10.1109/TPS.2013.2263255.
[25] A. M. Chaly, K. K. Zabello, and S. M. Shkol'nik, "Cathode spot velocity in tangential magnetic field on cathode of copper-chromium composition in vacuum," in *Proc. 26th Int. Symp. Discharges Elect. Insul. Vac.*, Mumbai, India, Sep./Oct. 2014, pp. 229–232.
[26] M. S. Benilov, "The Child–Langmuir law and analytical theory of collisionless to collision-dominated sheaths," *Plasma Sources Sci. Technol.*, vol. 18, no. 1, pp. 014005-1–014005-14, 2009. [Online]. Available: http://stacks.iop.org/0963-0252/18/014005
[27] D. Bohm, "Minimum ionic kinetic theory for a stable sheath," in *The Characteristics of Electrical Discharges in Magnetic Fields*, A. Guthrie and R. K. Wakerling, Eds. New York, NY, USA: McGraw-Hill, 1949, pp. 77–86.
[28] M. S. Benilov and L. G. Benilova, "The double sheath on cathodes of discharges burning in cathode vapour," *J. Phys. D: Appl. Phys.*, vol. 43, no. 34, pp. 345204-1–345204-12, 2010. [Online]. Available: http://stacks.iop.org/0022-3727/43/i=34/a=345204

Mikhail S. Benilov received the Diploma degree (Hons.) and the C.Sc. (Ph.D.) degree in physics from the Moscow Institute for Physics and Technology, Moscow, Russia, in 1974 and 1978, respectively, and the Doctor of Physical and Mathematical Sciences degree from the Institute for High Temperatures, USSR Academy of Sciences, Moscow, in 1990. His thesis focuses on the theory of electrostatic probes and electrodes in high-pressure flowing plasmas.

After completing postgraduate courses at the Moscow Institute for Physics and Technology and the Institute for Mechanics, Lomonosov Moscow State University, Moscow, in 1977, he was with the Institute for High Temperatures, USSR Academy of Sciences, where he led a group working in plasma and nonlinear physics, numerical modeling, and fluid dynamics. Since 1993, he has been a Professor with the Department of Physics, University of Madeira, Funchal, Portugal. His current research interests include plasma physics, in particular, plasma–electrode interaction, kinetic theory of phase transitions, and numerical modeling.

Dr. Benilov received the Alexander von Humboldt Research Fellowship in 1990 and stayed for two years with the Ruhr-Universität Bochum, Germany, working on the theory and simulation of near-electrode phenomena.

Helena T. C. Kaufmann received the M.Sci. degree in physics from the Imperial College of Science, Technology and Medicine, London, U.K., in 2012, and the Ph.D. degree in physics from the University of Madeira, Funchal, Portugal, in 2019. Her thesis focuses on the plasma–cathode interaction in vacuum and unipolar arcs, in particular, on the numerical modeling of cathode spots and related phenomena in vacuum arc discharges, and the applicability of similar concepts and modeling to unipolar arcs in fusion-relevant conditions.

Her current research interests include plasma–electrode interaction in arc discharges and numerical modeling.

Werner Hartmann received the M.S. degree in physics and the Ph.D. degree from the University of Erlangen-Nuremberg, Erlangen, Germany, in 1981 and 1986, respectively.

From 1986 to 1991, he was a Research and Teaching Assistant with the Physics Department, University of Erlangen-Nuremberg. From 1987 to 1988, he was with the University of Southern California at Los Angeles, Los Angeles, CA, USA, where he conducted research on cold cathode thyratrons/pseudosparks and fast dynamic z-pinches as EUV light sources. Since 1991, he has been a Researcher, a Research Group Leader, a Project Manager, and a Program Manager with Siemens Corporate Technology. He was responsible for fundamental and applied research into vacuum switching arc physics and devices with the Corporate Technology of Siemens, being involved in the development of low-voltage contactors, low-voltage circuit breakers up to 130 kA breaking capacity, medium voltage vacuum circuit breakers, and the successful development of high-voltage vacuum circuit breakers for 72 and 145 kV. He was involved in the development of a fully 3-D, fully transient software code for the simulation of low-voltage switching arcs in the air as a Project Manager. He developed environmental and environmentally friendly technologies for industrial applications, mainly in the areas of clean water, clean air, and electroporation. He held the position of a Senior Key Expert in the area of environmental technologies. His research interests include the field of mining applications, particularly in the field of flotation and magnetic separation.

Dr. Hartmann passed away prematurely in 2017.

Larissa G. Benilova received the Diploma degree in electrical engineering from the Moscow Institute of Railway Engineering, Moscow, Russia, in 1975.

From 1975 to 1996, she was with several computing centers in Moscow, and Bochum, Germany. From 1997 to 1999, she was with the Instituto Superior Técnico, Lisbon, Portugal, where she was involved in the area of scientific programming and word processing. Since 2001, she has been an Engineer–Programmer with the Universidade da Madeira, Funchal, Portugal, performing scientific programming and numerical simulations in the framework of a number of research projects in plasma science and applications funded by the European Union, the Fundação para a Ciência e a Tecnologia of Portugal, and international industry. She has authored or co-authored a number of papers in research journals and conference proceedings.